

Experimental observation of high-order quantum accelerator modes

S. Schlunk,¹ M.B. d’Arcy,¹ S.A. Gardiner,¹ and G.S. Summy^{1,2}

¹Clarendon Laboratory, Department of Physics, University of Oxford, Parks Road, Oxford, OX1 3PU, United Kingdom

²Department of Physics, Oklahoma State University, Stillwater, Oklahoma, 74078-3072

(Dated: December 25, 2021)

Using a system consisting of a freely falling cloud of cold cesium atoms periodically kicked by pulses from a vertical standing wave of laser light, we present the first experimental observation of high-order quantum accelerator modes. This confirms the recent prediction by Fishman, Guarneri, and Rebuzzini [Phys. Rev. Lett. **89**, 084101 (2002)]. We also show how these accelerator modes can be identified with the stable regions of phase space in a classical-like chaotic system, despite their intrinsically quantum origin.

PACS numbers: 05.45.Mt, 03.65.Sq, 32.80.Lg, 42.50.Vk

The search for signatures of chaos and stability in quantum systems whose classical analogs can exhibit chaotic dynamics is an area of intense current theoretical and experimental interest. The motivation for such investigations is twofold. Firstly, the study of the way in which complex classical behaviour has its origin in the quantum regime helps in understanding the operation of the quantum-classical correspondence principle and thus the physical processes that are crucial in determining observed macroscopic behaviour, particularly when this behaviour is unpredictable and chaotic. Secondly, the quantum dynamics of such systems are of considerable interest in their own right, especially when the systems behave in a peculiarly non-classical manner.

The study of quantum chaos and stability has focused on both energetic and dynamical properties of systems [1, 2, 3, 4]. Approaches to the classification of quantum systems’ behaviour have ranged from the highly mathematical (e.g. trace formulae [2]) through the statistical (energy spectra [3]) to the more phenomenological (energy and momentum transfer to ensembles of particles [4]). It is the latter approach which is most appealing as a philosophy to guide experimental investigations, and has underpinned the work presented in this Letter. Resonant, stable behaviour in quantum systems often depends on precise fulfilment of matching conditions between periodic forcing of a system and its own natural frequency. This is in stark contrast to the looser matching which is generally required in the corresponding classically chaotic system [5]. The quantum resonances [6] observed in the δ -kicked rotor [7, 8] represent an excellent example of this dichotomy between the quantum and the classical. These resonances are characterised by the steady transfer of momentum to the system, which in the atom-optical case [9, 10] manifests itself as a symmetric broadening of the atomic momentum distribution for special values of the driving frequency of the potential. This phenomenon is therefore interesting in terms of both the motivations outlined above.

In this Letter, we report the results of experiments using an atom-optical realization [11] of the δ -kicked accelerator [12, 13, 14, 15]. This is realized when pulses from a vertical standing wave of laser light are applied to freely falling laser-cooled atoms. The Hamiltonian for this system is given by

$$\hat{H} = \frac{\hat{p}^2}{2m} + mg\hat{z} - \hbar\phi_d[1 + \cos(G\hat{z})] \sum_n \delta(t - nT), \quad (1)$$

which is related to the classically chaotic δ -kicked rotor by the addition of a static linear potential. Here \hat{z} is the position, \hat{p} the momentum, m the particle mass, g the gravitational acceleration, t the time, T the pulse period, $G = 2\pi/\lambda_{\text{spat}}$, where λ_{spat} is the spatial period of the potential applied to the atoms, and $\hbar\phi_d$ quantifies the depth of this potential. The classical dynamics of this system are qualitatively similar to those of the δ -kicked rotor, whereas the quantum dynamics are quite distinct. For example, the quantum accelerator modes recently discovered in this system [12] are not observed in the corresponding classical system. The modes are characterised by the asymmetric transfer of a fixed momentum impulse per kick to approximately 20% of the initial ensemble of laser-cooled atoms. In a recent analysis of this phenomenon by Fishman, Guarneri, and Rebuzzini (FGR) [5], quantum accelerator modes were interpreted as being a resonant type of behavior, closely related to the quantum resonances in the δ -kicked rotor. This analysis also led to the fascinating prediction of the existence of whole families of higher-order quantum accelerator modes. These were shown to correspond to higher-order fixed points centered on systems of islands in a (pseudo)classical phase space. In this Letter we report the first experimental observation of these higher-order accelerator modes, finding excellent quantitative agreement with the analysis of Ref. [5].

The kicking potential acts on the atoms as a phase grating that induces a phase modulation of amplitude ϕ_d to their de Broglie waves. Hence the effect of a pulse on a plane wave is to cause diffraction into a series of momentum states separated by the grating recoil $\hbar G$. Between consecutive pulses these states accumulate a phase related to their kinetic energy. This phase evolution is determined by the value of T , which will therefore govern the type of dynamics exhibited by the system. As in Refs. [14, 15], we use scaled position and momentum variables $\chi = Gz$ and $\rho = GTp/m$. An effective scaled, dimensionless Planck constant $\hbar = \hbar G^2 T/m$ is then defined through the relation $\hbar = -i[\hat{\chi}, \hat{\rho}]$. This parameter, together with ϕ_d and $\gamma = gGT^2$ (which accounts

for the effect of gravity) fully describe the quantum dynamics of the δ -kicked accelerator. When quantum resonances occur in the δ -kicked rotor ($\gamma = 0$), the phase difference accumulated between momentum states separated by $\hbar G$ from one pulse to the next is equal to an integer multiple of 2π . For a state of zero initial momentum, this is the case for values of T corresponding to $\hbar k = 4\pi\ell$ where $\ell \in \mathbb{Z}$. This rephasing is analogous to the Talbot effect in optics [16], and so we speak of these resonances as occurring at integer multiples of the Talbot time $T_T = 4\pi m/\hbar G^2$ [13]. For a continuous initial distribution of momenta, such as in a cold atomic ensemble, resonant behavior is observed for $\hbar k = 2\pi\ell$, i.e. at integer multiples of the half-Talbot time, $T_{1/2}$ [9, 10, 14]. Close to these values of T , quantum accelerator modes are found in the δ -kicked accelerator [14].

In our experimental realization of the quantum δ -kicked accelerator, about 10^7 caesium atoms are trapped and cooled in a magneto-optic trap (MOT) to a temperature of $5\mu\text{K}$, yielding a Gaussian momentum distribution with FWHM $6\hbar G$. The atoms are then released from optical molasses and, falling freely under gravity, are exposed to pulses from a vertical standing wave of off-resonant laser light that is 20 GHz red-detuned from the $6^2\text{S}_{1/2} \rightarrow 6^2\text{P}_{1/2}$, ($F = 4 \rightarrow F' = 3$) D1 transition. Hence $\lambda_{\text{spat}} = 447\text{ nm}$ and $T_{1/2} = 66.7\mu\text{s}$. The intensity of the light in each pulse is approximately $1 \times 10^8\text{ W/cm}^2$, and the duration of each pulse is 500 ns. Through the action of the ac Stark shift, these pulses result in δ -function-like applications of a spatially periodic potential to the atoms, with $\phi_d = \Omega^2 t_p / 8\delta_L$. Here Ω is the Rabi frequency, t_p the duration of each (square) pulse and δ_L the detuning from the D1 transition. Both the trapped atom density distribution and the standing light wave intensity profile are Gaussian, with full width at half maximum (FWHM) of 1 mm. The resulting mean value of ϕ_d is around 0.8π . After application of the diffracting pulses, the atoms fall through a sheet of light resonant with the $6^2\text{S}_{1/2} \rightarrow 6^2\text{P}_{3/2}$, ($F = 4 \rightarrow F'' = 5$) D2 transition, located 0.5m below the point of release, and their momentum distribution is measured by a time-of-flight technique with a resolution of $\sim \hbar G$. For more details regarding our experimental setup see Refs. [13, 14, 15].

The approach used by FGR [5] accounts for the observed acceleration of atoms participating in a quantum accelerator mode in terms of stable fixed points in a map for a classical point particle. The validity of this map can be justified asymptotically by the closeness of $\hbar k$ to integer multiples of 2π . The pseudoclassical limit can be described by $\epsilon = (\hbar k - 2\pi\ell) \rightarrow 0$ (hence the description ‘pseudoclassical’), or equivalently by $(\ell - T/T_{1/2}) \rightarrow 0$. In an appropriately transformed frame [5], the map is given by [15]

$$\tilde{\rho}_{n+1} = \tilde{\rho}_n - \tilde{k} \sin(\chi_n) - \text{sign}(\epsilon)\gamma, \quad (2)$$

$$\chi_{n+1} = \chi_n + \text{sign}(\epsilon)\tilde{\rho}_{n+1}, \quad (3)$$

where $\tilde{\rho} = \rho\epsilon/\hbar k$, and $\tilde{k} = \phi_d|\epsilon|$. With the correct initial conditions, iteration of Eqs. (2) and (3) yields systems of accelerator orbits. These are stable fixed points centered on islands in

the pseudoclassical phase space. To yield an observable quantum accelerator mode an island system must be sufficiently large, in terms of total phase-space area. Thus, in a classical sense, the islands must encompass sufficient phase space density for the accelerator mode to be measurable. Furthermore, the islands must be large, or at least comparable to $|\epsilon|$ (which takes the place of \hbar as a measure of the size of a minimal ‘quantum phase space’ cell) for a point particle-like description of the quantum accelerator mode dynamics to be appropriate. We show in this Letter that when these requirements are satisfied, the momentum gain predicted by the analysis of FGR agrees very well with experiment, even when $\hbar k$ is not extremely close to a resonant value. This can be understood as being due to the relevant dynamics taking place in stable regions of the pseudoclassical phase space, where semiclassical analyses can generally be expected to work reasonably well [17].

FGR [5] classify accelerator orbits (and thus quantum accelerator modes) by the order \mathbf{p} of the fixed point (i.e. how many pulse periods it takes before cycling back to the initial point in the reduced phase space cell) and the jumping index \mathbf{j} (related to how many units of the momentum period of phase space are imparted to the accelerating atoms per cycle). Particles in a pseudoclassical (\mathbf{p}, \mathbf{j}) mode with an initial momentum of $q_0\hbar G$ have, after N kicks, a momentum (in units of $\hbar G$) given by

$$q \simeq q_0 + \frac{N}{|\ell - T/T_{1/2}|} \left[\frac{\mathbf{j}}{\mathbf{p}} + \text{sign}(\ell - T/T_{1/2}) \frac{\gamma}{2\pi} \right], \quad (4)$$

in a frame accelerating with gravity. Only atoms of certain initial momenta will be accelerated [13]; ideal values of q_0 and initial position can be determined analytically [5]. As our molasses-cooled atomic ensemble extends over many phase space cells, all such conditions can be satisfied. All atoms fulfilling these conditions will receive the same momentum transfer. Since the mean initial momentum is 0, the central momentum of the observed accelerator mode is well described by Eq. (4) with $q_0 = 0$.

To search for high-order accelerator modes, we measured the momentum distribution after a fixed number of pulses for a range of T in the vicinity of the first three integer multiples of $T_{1/2}$. Figure 1 displays the experimental momentum distributions after 30 pulses for values of T in the region of (a) $T_{1/2}$ ($T = 60.5\mu\text{s}$ to $74.5\mu\text{s}$), (b) $T_T = 2T_{1/2}$ ($124.5\mu\text{s}$ to $142.5\mu\text{s}$), and (c) $3T_{1/2}$ ($191.5\mu\text{s}$ to $209.5\mu\text{s}$). The dotted curves indicate the theoretical predictions of Eq. (4). There is some disagreement for very large momenta, particularly large negative momenta. At these momenta, the atoms have left the Raman-Nath regime [14], and move so quickly that they travel a significant fraction of the standing wave period λ_{spat} during a pulse. These atoms experience a spatially averaged potential, so it is no longer appropriate to speak of δ -function-like kicks. Such an effect will be stronger for atoms accelerated in the negative direction (*with* gravity) than in the positive (*against* gravity).

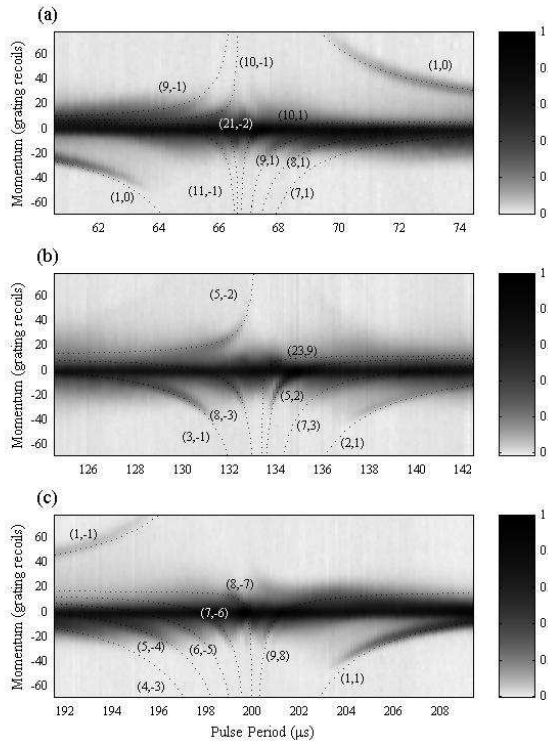


FIG. 1: Pseudocolor plots of the variation with T of the experimental momentum distribution after 30 kicks, in a frame falling freely with gravity. The value of T was varied around (a) $T_{1/2}$, (b) $T_T = 2T_{1/2}$, and (c) $3T_{1/2}$, in steps of $0.128\mu\text{s}$. The overlaid dotted lines indicate the predicted momenta [Eq. (4)] of selected quantum accelerator modes, labelled by (\mathbf{p}, \mathbf{j}) .

Certain of the more slowly accelerating (higher-order) quantum accelerator modes can only be resolved after applying a larger number of pulses than used in Fig. 1. To observe the emergence of several such modes, the value of T was scanned, for larger pulse numbers, in the region of T_T . Figure 2 shows the experimental momentum distributions after (a) 60, (b) 90, (c) 120, and (d) 150 pulses. Overlaid white lines indicate the predictions of Eq. (4). In Fig. 2(a) we can now identify the $(13, -5)$ and $(23, 9)$ modes. After 90 kicks [Fig. 2(b)] the $(18, -7)$ accelerator mode is emerging, whereas the momenta of the $(2, 1)$ and the $(5, -2)$ modes have grown beyond the measurable range. In Figs. 2(c) and 2(d) the atoms have received yet more momentum, and the $(3, -1)$ mode is no longer visible. Note also that some of the quantum accelerator modes seem to ‘fade’ and become diffuse with time; this effect is not predicted by the pseudoclassical model and may be due to tunneling [5].

We now explicitly connect the experimentally observed higher-order quantum accelerator modes around T_T , as displayed in Figs. 1(b) and 2, with their corresponding island systems in pseudoclassical phase space. Figure 3 shows strobo-

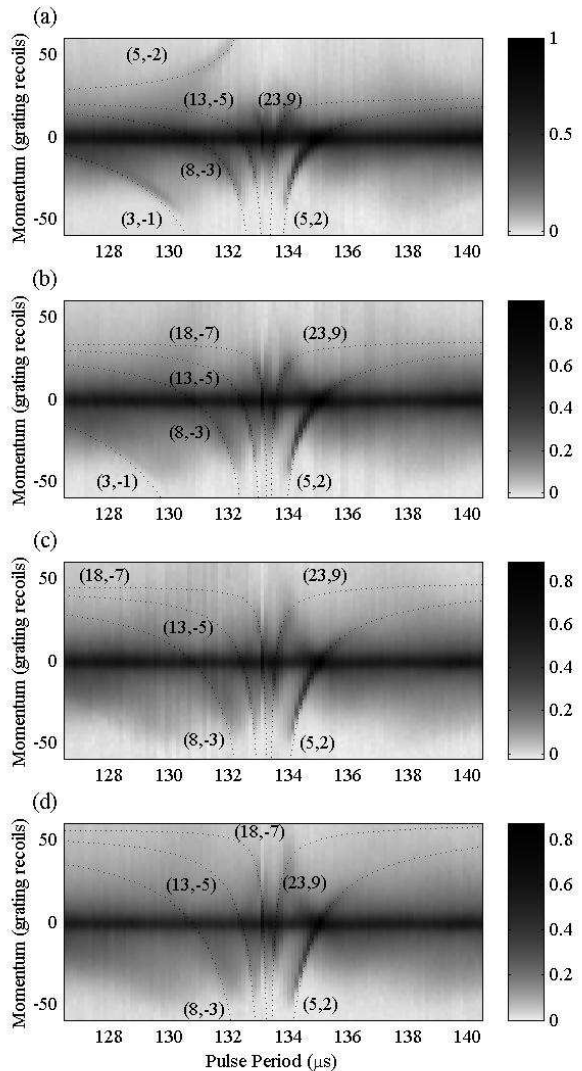


FIG. 2: Experimental momentum distributions for different pulse numbers as T is varied in the vicinity of the Talbot time $T = T_T$, from $124.5\mu\text{s}$ to $142.5\mu\text{s}$ in steps of $0.128\mu\text{s}$. The total pulse number is (a) 60, (b) 90, (c) 120, and (d) 150. The overlaid dotted lines indicate the predicted momenta [Eq. (4)] of selected quantum accelerator modes, labelled by (\mathbf{p}, \mathbf{j}) .

scopic phase space plots, generated numerically by repeated iterations of Eqs. (2) and (3), for different values of T around T_T . The island systems can be identified with the experimentally observed quantum accelerator modes. Comparing Figs. 2 and 3, we see that the appearance and disappearance of the quantum accelerator modes and of the stable island systems as T is varied coincide. Figure 3(a) ($T = 130.0\mu\text{s}$) shows the three large islands corresponding to the $(3, -1)$ quantum accelerator mode. In Fig. 3(b) it is possible to observe the coexis-

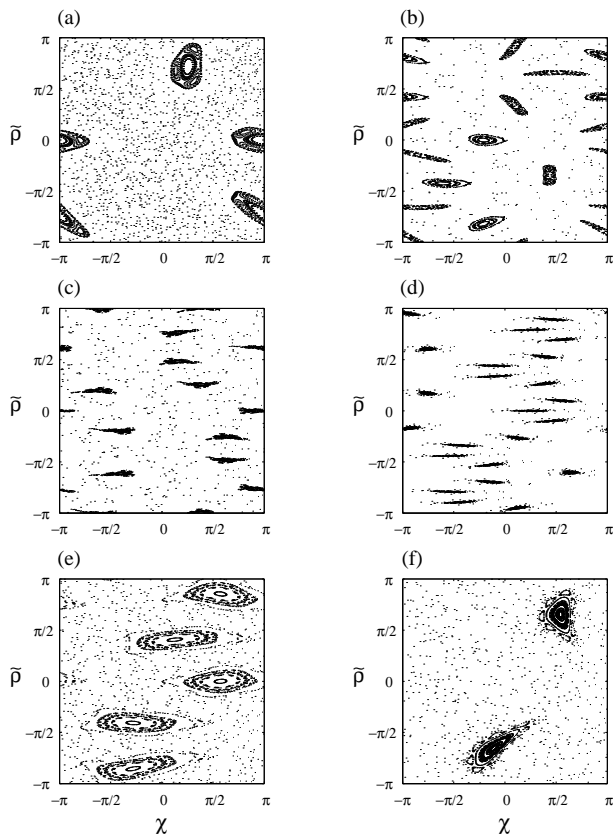


FIG. 3: Phase space plots produced by the (pseudo)classical map of Eqs. (2) and (3) for values of T close to the Talbot time T_T . The islands correspond to the following quantum accelerator modes: (a) $T = 130.0\mu\text{s}$, and $(\mathbf{p}, \mathbf{j}) = (3, -1)$; (b) $T = 132.2\mu\text{s}$, $(\mathbf{p}, \mathbf{j}) = (5, -2)$ (shorter, rounder islands) and $(8, -3)$ (thin, elongated islands); (c) $T = 132.8\mu\text{s}$, $(\mathbf{p}, \mathbf{j}) = (13, -5)$; (d) $T = 133.5\mu\text{s}$, $(\mathbf{p}, \mathbf{j}) = (23, 9)$; (e) $T = 134.2\mu\text{s}$, $(\mathbf{p}, \mathbf{j}) = (5, 2)$; and (f) $T = 139.4\mu\text{s}$, $(\mathbf{p}, \mathbf{j}) = (2, 1)$. We have clustered the initial conditions around the fixed points corresponding to accelerator orbits to highlight the structure of the island system of interest.

tence of a $(5, -2)$ and a $(8, -3)$ island system at $T = 132.2\mu\text{s}$, which can be seen to be consistent with the experimental results in Figs. 1(b) and 2(a). Interestingly, these yield simultaneous momentum transfer in opposite directions, promising application as a beam-splitting technique. Figure 3(c) ($T = 132.8\mu\text{s}$) shows the emergence of a $(13, -5)$ accelerator orbit, while in Fig. 3(d) we see a complex $(23, 9)$ island system at $T = 133.5\mu\text{s}$ (just greater than T_T). This nevertheless appears to correspond to a fairly robust quantum accelerator mode that is clearly visible in each of the subplots of Fig. 2. Moving further away from T_T , in Figs. 3(e) and 3(f) ($T = 134.2\mu\text{s}$ and $139.4\mu\text{s}$, respectively), we again observe comparatively simple orbits, $(5, 2)$ and $(2, 1)$, respectively.

In conclusion, we have successfully observed a multitude of quantum accelerator modes of up to 23rd order, and connected them to the periodic orbits of a classical map. This was derived by FGR [5] as a pseudoclassical limit of the underlying

quantum dynamics when the pulse period approaches certain resonance times. Linking this theory with our experiment, we have successfully performed quantum accelerator mode spectroscopy. Confirmation of the validity of such a theoretical approach promises new avenues for investigation of quantum-classical correspondence in a chaotic context. Furthermore, the efficient momentum transfer occurring in these atomic dynamics is of great intrinsic interest. We have recently demonstrated quantum accelerator modes to be formed coherently [15], and the simultaneous existence of quantum accelerator modes in opposite momentum directions could be applied as a beam-splitter for large-area atom interferometry [18].

We thank R. Bach, K. Burnett, S. Fishman, I. Guarneri, L. Rebuzzini, and S. Wimberger for stimulating discussions. We acknowledge support from the UK EPSRC, the Paul Instrument Fund of The Royal Society, the EU as part of the TMR ‘Cold Quantum Gases’ network, contract no. HPRN-CT-2000-00125, the DAAD (S.S.), and the Royal Commission for the Exhibition of 1851 (M.B.d’A.).

-
- [1] H.-J. Stöckmann, *Quantum Chaos: an introduction* (Cambridge University Press, Cambridge, 1999); *New Directions in Quantum Chaos*, edited by G. Casati, I. Guarneri, and U. Smilansky (IOS Press, Amsterdam, 2000).
 - [2] M.C. Gutzwiller, *Chaos in Classical and Quantum Mechanics* (Springer-Verlag, New York, 1990)
 - [3] F. Haake, *Quantum Signatures of Chaos* (2nd ed.) (Springer-Verlag, Berlin, 2001).
 - [4] L.E. Reichl, *The Transition to Chaos in Conservative Classical Systems: Quantum Manifestations* (Springer-Verlag, New York, 1992).
 - [5] S. Fishman, I. Guarneri, and L. Rebuzzini, Phys. Rev. Lett. **89**, 084101 (2002); e-print nlin.CD/0202047.
 - [6] F.M. Izrailev and D.L. Shepelyanskii, Sov. Phys. Dokl. **24**, 996 (1979).
 - [7] A.L. Lichtenberg and M.A. Lieberman, *Regular and Chaotic Dynamics* (Springer-Verlag, Berlin, 1992); G. Casati *et al.*, in *Stochastic Behaviour in Classical and Quantum Hamiltonian Systems*, (Springer-Verlag, New York, 1979).
 - [8] F.L. Moore, *et al.*, Phys. Rev. Lett. **75**, 4598 (1995).
 - [9] W.H. Oskay *et al.*, Opt. Commun. **179**, 137 (2000).
 - [10] M.B. d’Arcy *et al.*, Phys. Rev. Lett. **87**, 074102 (2001).
 - [11] B.G. Klappauf, *et al.*, Phys. Rev. Lett. **81**, 1203 (1998); H. Ammann *et al.*, *ibid* **80**, 4111 (1998); M.B. d’Arcy *et al.*, *ibid* **87**, 074102 (2001); W.K. Hensinger *et al.*, Nature (London) **412**, 52 (2001); D.A. Steck, W.H. Oskay, and M.G. Raizen, Science **293**, 274 (2001).
 - [12] M.K. Oberthaler *et al.*, Phys. Rev. Lett. **83**, 4447 (1999).
 - [13] R.M. Godun, *et al.*, Phys. Rev. A **62**, 013411 (2000).
 - [14] M.B. d’Arcy *et al.*, Phys. Rev. E **64**, 056233 (2001).
 - [15] S. Schlunk *et al.*, e-print physics/0207075.
 - [16] See also related work on classical optics by M.V. Berry and E. Bodenschatz, J. Mod. Opt. **46**, 349 (1999).
 - [17] W.H. Zurek and J.P. Paz, Phys. Rev. Lett. **72**, 2508 (1994).
 - [18] P. Berman, *Atom Interferometry* (Academic Press, San Diego, 1997).